Preprints of the 19th World Congress
The International Federation of Automatic Control
Cape Town, South Africa. August 24-29, 2014

Model Reduction and Control of a Compressible Channel Flow with Combustion ⋆

Lorenz Pyta * **Mathias Hakenberg** * **Dirk Abel** *

* *Institute of Automatic Control RWTH Aachen University, Aachen 52074 , Germany, L.Pyta@irt.rwth-aachen.de.*

Abstract: A model reduction for a compressible flow with combustion is performed using the POD-Galerkin procedure. The model parameters are determined by an optimization. The obtained reduced-order model is incorporated in a model predictive controller and results are shown from a closed-loop CFD-simulation. The controller influences the fuel mass-flow boundary condition to control the temperature at a certain point within the computational domain.

1. INTRODUCTION

In many types of combustion processes, e.g. a combustion in a rotary kiln for cement production, it is important to guarantee a constant temperature profile over time. This will be hard to achieve if the fuel mass flow for the combustion has a changing heat value. This may occur if waste is used for the combustion in order to reduce the use of expensive fossil fuels. Thus a controller is needed to keep the temperature profile constant.
Modeling this types of combustion processes requires the consideration of the spatial extension of the system states. Systems with non-negligible spatial dimension are called distributed parameter systems and are typically modeled with partial differential equations (PDEs) e.g. the Navier-Stokes-Equations for flow problems. However, designing a feedback controller requires low dimensional models of ordinary differential equations (ODEs). One established approach to retrieve an ODE-Model from a PDE is the Proper Orthogonal Decomposition (POD) and subsequent Galerkin projection (see e.g. Holmes et al. [1996]). The idea is to compute a set of spatial basis functions of a subspace containing most information from empirical data and to project the PDE onto this subspace to arrive an ODE.
These methods have been applied in many different cases of flow control. Kunisch and Volkwein [1999] obtained a reduced model for the Burgers Equation via POD-Galerkin technique. The empirical data for building up the model has been generated from simulations. Baker and Christofides [1999] analyzed the incompressible two-dimensional Navier-Stokes equations in order to describe Newtonian fluids and to synthesize a nonlinear controller. The actuation has been realized via a volume force in the equations. A case with three dimensions was examined by Ma and Karniadakis [2002], who investigated the flow past a cylinder by proper orthogonal decomposition to reproduce the arising limit cycle. For the Galerkin projection the incompressible Navier-Stokes equations were used.
In all these approaches the flow is considered incompressible, which simplifies the Navier-Stokes equations and the simulations needed to obtain the data for the POD. However, combustion processes like all processes with noteworthy temperature changes, require compressible modeling. An investigation of the two-dimensional compressible Navier-Stokes-Equations has been given by Iollo et al. [2000]. They formulated a compressible Galerkin-model with conservation equations in velocity, pressure and specific volume. Heat flow was not considered. The choice of specific volume instead of density guarantees a polynomial structure of the model. A compressible case is also covered in Gloerfelt [2008]. The POD is applied in order to describe flow oscillations in a cavity. Again the specific volume is chosen as value for the conservations equations and the Galerkin projection. Some additional techniques for compressible POD have been introduced by Rowley et al. [2004]. They used simplified isentropic but compressible Navier-Stokes equations for the Galerkin-projection and modified the inner product for the projection in order to respect both thermodynamic and kinematic variables.
An approach to include actuation via changing boundary conditions in the reduced order model was outlined by Graham et al. [1999]. They introduced an additional mode, which homogenizes the given data ensemble at every time step and thus represents the boundary conditions.
The POD-Galerkin method delivers the structure of the model and the corresponding coefficients of the model. As the computation of the modes requires empirical data of the process, the calculation of the coefficients depends on the modes and their derivatives, which can lead to numerical problems. In order to improve the accuracy of the reduced models, Couplet et al. [2005] and also Cordier et al. [2009] calibrated the coefficients of the model using optimization methods and regularizations.

In the present paper the outlined knowledge is combined to receive a reduced model via the POD-Galerkin method for a compressible channel flow with combustion. For that purpose the models in Gloerfelt [2008] are expanded with a combustion term to consider the heat flow. Actuation via boundary conditions is considered using the 'control function' approach of Graham et al. [1999]. The model is calibrated with the tools introduced in Cordier et al.

⋆ The authors gratefully acknowledge funding from the German Research Foundation (DFG) for the Research Unit 'Active Drag Reduction' (AB65/12-1).

[2009]. A model predictive controller is set up using the reduced model to control the temperature inside the channel at a specific point. Section 2 introduces the plant. Section 3 gives a short overview over the POD-Galerkin method, while the actual reduced order model is derived in Section 4. The controller design is described in Section 5 connected with the investigation of the controller's performance. Section 6 gives a short conclusion.

2. SIMULATION AND PLANT

The plant considered in this paper is a compressible channel flow with combustion simulated with the CFD-Solver Fluent from ANSYS [2011]. In order to simplify computations and to utilize symmetry, the upper half of a longitudinal cut through a channel of 50 m length and a height of 5 m is considered as plant. Thus the computation area is two-dimensional with a length of 50 m and a height of 2.5 m. For further modeling only two dimensions have to be taken into account.
The fuel inlet with a height of 12.5 cm, where methane enters the channel with a constant temperature of 300 K, is located on the lower part of left boundary. The mass flow of methane is variable and can be actuated by the controller. Preheated air with a mass flow of 21.6 kg/s enters the channel at a constant temperature of 973 K through the upper part of the left boundary. The velocity vanishes on the walls along the channel and heat transfer across the wall is also considered. On the right side of the channel a pressure outlet condition with a gauge pressure of 1 bar is used.
A sketch of the plant is shown in Fig. 1.

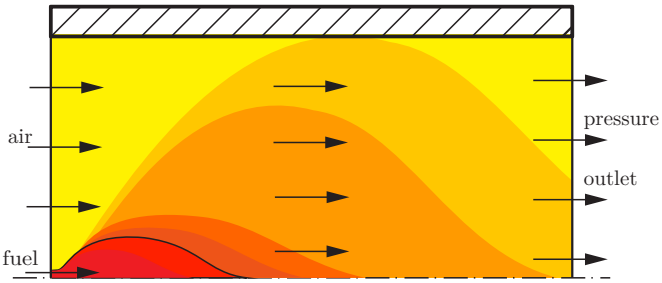

Fig. 1. Boundary conditions of the plant

The physics of the channel-flow are described by the conservation of mass, conservation of momentum and conservation of energy. The equation for conservation of mass can be written as

$$\frac{\partial}{\partial t}\rho + \operatorname{div}(\rho \boldsymbol{v}) = 0 \tag{1}$$

for the whole system and (without concerning mass diffusion)

$$\frac{\partial}{\partial t}(\rho Y_k) + \operatorname{div}(\rho Y_k \boldsymbol{v}) = \dot{\omega}_k \tag{2}$$

for every species, where ρ denotes the density, $\boldsymbol{v}$ the velocity, Y_k the mass fraction of species and $\dot{\omega}_k$ the generation rate of species k. Further the reaction of species is described by

$$CH_4 + 2\ O_2 \Rightarrow CO_2 + 2\ H_2O. \tag{3}$$

The conservation of momentum becomes with $\boldsymbol{v} = (\boldsymbol{v}_1\ \boldsymbol{v}_2)^{\mathrm{T}} = (u\ v)^{\mathrm{T}}$

$$\frac{\partial}{\partial t}(\rho u) + \operatorname{div}(\rho u \boldsymbol{v}) = -\frac{\partial p}{\partial x_1} + \frac{\partial \tau_{11}}{\partial x_1} + \frac{\partial \tau_{21}}{\partial x_2} \tag{4}$$

in streamwise direction x_1 and

$$\frac{\partial}{\partial t}(\rho v) + \operatorname{div}(\rho v \boldsymbol{v}) = -\frac{\partial p}{\partial x_2} + \frac{\partial \tau_{12}}{\partial x_1} + \frac{\partial \tau_{22}}{\partial x_2} \tag{5}$$

in normal direction x_2. In these equations p denotes the pressure and τ_{ij} the stress tensor computed by

$$\begin{aligned} \tau_{11} &= \mu\left(\frac{4}{3}\frac{\partial}{\partial x_1}u - \frac{2}{3}\frac{\partial}{\partial x_2}v\right) \\ \tau_{22} &= \mu\left(\frac{4}{3}\frac{\partial}{\partial x_2}v - \frac{2}{3}\frac{\partial}{\partial x_1}u\right) \\ \tau_{12} = \tau_{21} &= \mu\left(\frac{\partial}{\partial x_2}u + \frac{\partial}{\partial x_1}v\right) \end{aligned} \tag{6}$$

with the dynamic viscosity μ.
In order to close the system of equations the ideal gas law

$$p = \rho R T \tag{7}$$

is applied. Here R denotes the specific gas constant and T the temperature of the gas. For the caloric state equation

$$e = c_v T \tag{8}$$

is used, where c_v is the isochoric heat capacity and e the internal energy.
Finally, the conservation of energy is described by

$$\begin{aligned} &\frac{\partial(\rho(e + \frac{\|\boldsymbol{v}\|^2}{2}))}{\partial t} + \operatorname{div}(\rho(e + \frac{\|\boldsymbol{v}\|^2}{2})\boldsymbol{v}) = -\operatorname{div}(\boldsymbol{v}p) \\ &+\Delta(kT)\ + \rho\dot{q}\ - \sum_{k=1}^{N} h_k \dot{\omega}_k\ + \sum_{i,j=1}^{2} \frac{\partial(\tau_{ij} v_j)}{\partial x_i} \end{aligned} \tag{9}$$

with $\dot{q}$ as the volumetric heat flow, the enthalpy of formation h_k and the thermal conductivity k.
These equations are solved by the CFD-Solver Fluent using an implicit pressure based solver with a Courant number of ten and a cell-based least square method to approximate the gradient. For turbulence the $k-\epsilon-$model was applied. The effects of radiation are considered using the P1-model. The input of the plant is the mass-flow of methane into the channel scaled with the nominal value 3 kg/s. The controlled variable is the cell average of the temperature at the position (20 m, 1.2 m).

For the model reduction dynamic information about the plant is needed in form of snapshots. These snapshots contain the data of different physical variables on the whole computational domain at certain points in time. To generate this snapshot-data the plant is simulated over a time scale of 15 s with a step size of 0.1 s for the data export. The 151 snapshots include all values of density, pressure, velocity and of mass-concentration of oxygen and methane. To generate dynamic information the plant has been simulated with an excitation of the left boundary condition. Fig. 2 shows the fuel mass flow at the inlet as a function of time. The mass-flow is scaled with the nominal value 2.5 kg/s and time is scaled by the cycle time.

3. REDUCED-ORDER-MODELS

The derivation of a reduced-order-model for a given plant with POD-Galerkin consists of two steps. The first is to compute a set of spatial basis functions via proper

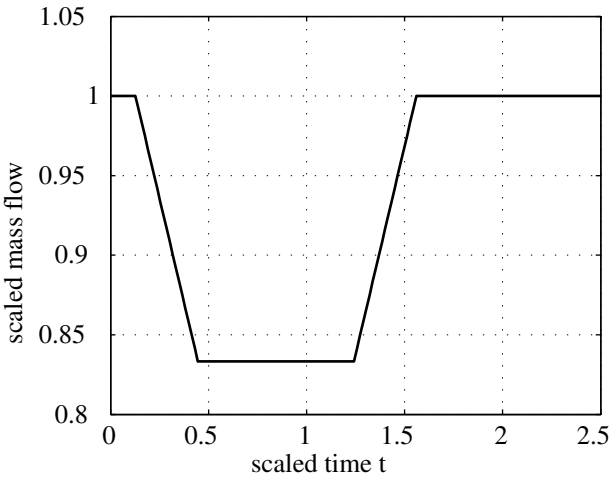

Fig. 2. Actuation of the plant

orthogonal decomposition based on the snapshot-data, which should cover the operating range of the system. Second the investigated PDE is reduced to a system of ODEs by application of the Galerkin-projection. Some theoretical background for the POD and the Galerkin-projection is outlined in paragraph 3.1 and 3.2. The model-reduction for the present case is presented in Section 4.

3.1 Proper Orthogonal Decomposition

Given a data set $y(t, \boldsymbol{x})$. The goal of the POD is to decompose the data into temporal coefficients $a_i(t)$ and spatial functions $\varphi_i(\boldsymbol{x})$ such that

$$y_N(t, \boldsymbol{x}) = \sum_{i=1}^{N} a_i(t)\varphi_i(\boldsymbol{x}) \tag{10}$$

is the optimal approximation of $y(t, \boldsymbol{x})$ in a time-averaged least-squares sense (see e.g. Holmes et al. [1996]). This problem leads to the determination of the spectrum of a linear, self-adjoint and compact operator. In case of time-discrete data and applying the method of snapshots introduced by Sirovich [1987] the solution simplifies to the calculation of eigenvalues of a correlation matrix.
Let $\langle \cdot, \cdot \rangle$ be a spatial inner product in $\mathrm{L}^2(\Omega)$ and N_t the number of time-steps in the data. Then the $(N_t \times N_t)$ correlation matrix can be computed by

$$C_{ij} = \langle y(t_i, \boldsymbol{x}) y(t_j, \boldsymbol{x}) \rangle. \tag{11}$$

The temporal coefficients $a_i(t)$ are determined as eigenvectors to the largest eigenvalues of C, hence

$$Ca_i = \lambda_i a_i. \tag{12}$$

The POD modes $\varphi_i(\boldsymbol{x})$ are given via projecting a_i on the data set y by

$$\varphi_i(\boldsymbol{x}) = \frac{1}{\sqrt{\lambda_i a^{\mathrm{T}} a}} a_i(t)^{\mathrm{T}} y(t, \boldsymbol{x}). \tag{13}$$

This computation ensures, that the POD modes form an orthonormal basis of an optimal subspace of $\mathrm{L}^2(\Omega)$. In the case that $y(t, \boldsymbol{x})$ is multi-dimensional the sum of the inner products of the different dimensions of y leads to the same result. For the compressible model reduction, different physical quantities like velocity or pressure need to be combined in one inner product. Therefore a proper scaling of the variables is essential to receive a meaningful decomposition. Here all variables will be scaled by the operating point values. So $y(t, \boldsymbol{x})$ has been scaled with the average values of the initial simulation. The calculation of POD modes ensures a model of low dimension and optimal representation of the ensemble data.

3.2 Galerkin-Projection

With this modal decomposition into temporal coefficients $a_i(t)$ and spatial basis functions $\varphi_i(\boldsymbol{x})$ a transformation of the PDE into a system of ODEs can be achieved. Substitution of the series expansion (10) into the PDE and projecting the residual onto the j-th basis function results in an ODE for the j-th temporal coefficient a_j. Repeating this procedure for each of the temporal coefficients gives a system of N ODEs. The corresponding calculation is the following: Given a PDE with the structure

$$\dot{y}(t, x) = f\left(y, \partial_x y, \ldots, \partial_x^n y\right). \tag{14}$$

From the Orthogonal Decomposition follows

$$y(t, \boldsymbol{x}) \approx \sum_{i=1}^{N} a_i(t)\varphi_i(\boldsymbol{x}) \quad \text{and} \quad \langle \varphi_i(x), \varphi_j(x) \rangle = \delta_{ij}, \tag{15}$$

where N is the number of POD modes. Then also the identity

$$\begin{aligned} \dot{a}_j &= \langle \dot{y}(t, x), \varphi_j(x) \rangle \\ &\approx \langle f\left(\sum_{i=1}^{N} a_i\varphi_i, \sum_{i=1}^{N} a_i\partial_x\varphi_i, \ldots, \sum_{i=1}^{N} a_i\partial_x^n\varphi_i\right), \varphi_j \rangle \\ &= \tilde{f}\left(a, \varphi, \partial_x\varphi, \ldots, \partial_x^n\varphi\right) \end{aligned} \tag{16}$$

holds. Boundary conditions do not explicitly occur in the resulting ODE-system. Thus for an exact matching of the boundary conditions, the boundary conditions have to be satisfied by the POD modes. This will only be the case for homogeneous boundary conditions, since the POD modes inherit these conditions from the data set and all linear combinations will fulfill them too. Inhomogeneous boundary conditions can be satisfied with additional modes introduced by Graham et al. [1999]

$$y(t, \boldsymbol{x}) = y_h(t, \boldsymbol{x}) + \bar{y}(\boldsymbol{x}) + u(t)\tilde{y}(\boldsymbol{x}). \tag{17}$$

Thereby $\bar{y}(\boldsymbol{x})$ meets the stationary boundary conditions while $\tilde{y}(\boldsymbol{x})$ represents the influence of the time dependent boundary condition $u(t)$. The POD is applied just on $y_h(t, \boldsymbol{x})$ and so these modes meet the homogeneous boundary conditions of $y_h(t, \boldsymbol{x})$. Thus the modes of y_h combined with $\tilde{y}(\boldsymbol{x})$ and $\bar{y}(\boldsymbol{x})$ fulfill the inhomogeneous boundary conditions.
The additional modes $\bar{y}(\boldsymbol{x})$ and $\tilde{y}(\boldsymbol{x})$ are in general not orthogonal to the POD modes of y_h and the equations are modified to

$$\dot{a}_j(t) = \langle \sum_{i=1}^{N} \dot{a}_i(t)\varphi_i(\boldsymbol{x}), \varphi_j(\boldsymbol{x}) \rangle - \dot{u}\langle \tilde{y}(\boldsymbol{x}), \varphi_j(\boldsymbol{x}) \rangle \tag{18}$$

and

$$\sum_{i=1}^{N} a_i(t)\varphi_i(\boldsymbol{x}) + \bar{y}(\boldsymbol{x}) + u(t)\tilde{y}(\boldsymbol{x}) = \sum_{i=1}^{N+2} a_i(t)\varphi_i(\boldsymbol{x}). \tag{19}$$

Because the input variable $\dot{u}$ appears as time-derivative in (18), its more convenient to choose

$$w = \dot{u} \tag{20}$$

as input of the system. The resulting model is a system of ODEs for the temporal coefficients $a_j(t)$ related to modes $\varphi_j(\boldsymbol{x})$ containing most information of the system dynamics. The j-the ODE of the model describes the change of the influence, that the mode $\varphi_j(\boldsymbol{x})$ has on the solution.

4. MODEL-REDUCTION OF THE CHANNEL-FLOW

At first some additional equations not directly included in the CFD-Simulation but needed for the reduction are presented. Together with the equations for the plant this results in a system of nonlinear PDEs, which will be reduced with the presented methods to a system of ODEs. Because direct calculation of the coefficients of the ODEs is ill conditioned, the structure of the reduced-order-model will be maintained, but the coefficients will be determined indirectly by an optimization.

4.1 Additional equations for the channel-flow

First methane (equivalent to $k = 1$), oxygen ($k = 2$) and $CO_2 + 2H_2O$ ($k = 3$) are chosen as species for equation (2) and (3). Further the kinetics of the reaction shall follow the differential equations

$$\begin{aligned} \frac{\partial}{\partial t}(\rho Y_1) &= -k_R \rho Y_1 \rho Y_2 \\ \frac{\partial}{\partial t}(\rho Y_2) &= -k_R \rho Y_2 \rho Y_1, \end{aligned} \tag{21}$$

where k_R is the rate constant. The change of the rate constant due to changes in temperature are describe by the Arrhenius ansatz, which presumes a exponential relation. The effects of radiation are described via the Stefan-Boltzmann law

$$\dot{q} = \frac{1}{V}\epsilon\sigma A T^4 \tag{22}$$

with the variables ϵ as the emissivity, σ the Stefan-Boltzmann constant and surface and volume A and V. Together with the equations (1) - (8) these form a system of nonlinear PDEs.

4.2 The reduced ODE-model

A direct Galerkin projection of the nonlinear PDEs into a reduced order model would lead to a model with terms of high order owing to the T^4-Term due to radiation and the e^T-Term due to the Arrhenius ansatz for the reaction coefficient. Also many physical quantities have to be taken to account. With the assumption, that k and R are constant, and via a linearization of the equation around a temperature working point T_0, the structure of the model can be simplified to an ODE-System with quadratic structure and only six physical quantities. These are the specific volume ξ, the streamwise and normal velocity u and v, the absolute pressure p and the mass concentrations of fuel ($\psi = \rho Y_1$) and oxygen ($\chi = \rho Y_2$). The choice of the inverse density (see Gloerfelt [2008]) ensures the polynomial structure of the resulting model, because the temperature can be written as $RT = p\xi$. With the choice of

$$\begin{aligned} y(t,\boldsymbol{x}) = (\xi\ u\ v\ p\ \psi\ \chi)^{\mathrm{T}} &= \left(y^I(t,\boldsymbol{x})\ \cdots\ y^{VI}(t,\boldsymbol{x})\right)^{\mathrm{T}} \\ \varphi_i(\boldsymbol{x}) &= \left(\varphi_i^I(\boldsymbol{x}) \cdots \varphi_i^{VI}(\boldsymbol{x})\right)^{\mathrm{T}} \end{aligned} \tag{23}$$

and the dot product

$$\langle y(\boldsymbol{x}), \varphi(\boldsymbol{x})\rangle = \sum_{i=I}^{VI} \langle y^i(\boldsymbol{x}), \varphi^i(\boldsymbol{x})\rangle \tag{24}$$

the resulting model has the structure

$$\begin{aligned} \dot{a}_j &= a^{\mathrm{T}}\left(\Xi^j + U^j + V^j + P^j + \Psi^j + X^j\right)a + w g_j \\ &= a^{\mathrm{T}} Q^j a + w g_j \quad \forall j = 1 \dots N \\ \dot{a}_{N+1} &= 0 \\ \dot{a}_{N+2} &= w. \end{aligned} \tag{25}$$

The states a_{N+1} and a_{N+2} correspond to the two homogenizing modes (the time average field and the actuation field). The matrices $\Xi^j \cdots X^j$ are related to the differential equations in ξ, u, v, p, ψ and χ and are computed by Galerkin projection (e.g. $\langle \dot{\xi}, \varphi_j^I\rangle \Rightarrow a^{\mathrm{T}}\Xi^j a$). Thereby the matrices include quadratic and also linear terms ($a_{N+1} = 1$). The term $g_j = -\langle \tilde{y}(\boldsymbol{x}), \varphi_j(\boldsymbol{x})\rangle$ represents the boundary control (see (18)). An example computation can be found in the appendix.

These equations include a computational scheme for the determination of the model-coefficients. However, for the computation of these coefficients, first order derivatives of the POD modes are required. Because of high pressure changes in the fuel inlet based on different velocities, this approach is numerical ill conditioned and delivers poor results. So it is more reasonable to identify the model-coefficients. However, the presented equations are used to define the structure of the reduced model, which is a system of quadratic ODEs.

4.3 Optimization of model-coefficients

A numeric practicable way to determine the model parameters of reduced Galerkin models has been introduced by Couplet et al. [2005]. The main idea is to demand, that the true coefficients - gathered by projection of the computed modes φ onto the solution data y - shall fulfill the differential equation. The optimization minimizes the quadratic error between that true coefficients and the result of the differential equation by changing the parameters of the differential equation. This approach has been applied by Cordier et al. [2009], who expanded the idea with an regularization. From the three different formulations presented in Cordier et al. [2009] the state calibration method

$$e_i(\zeta, t) = a_P^i(t) - \int_0^t f(\zeta_i, a_P(\tau))\mathrm{d}\tau - a_P^i(0), \tag{26}$$

where ζ denotes the optimization parameters and f the differential equation, has been chosen. The resulting linear equation system has been regularized using the Tikhonov method in order to reduce the condition number to an acceptable value. Only half of the simulation time was used for identification of the model parameters, the other half was used for validation. The training-data span the non-dimensional timescale from 1 to 2 (scaled with a cycle time of 6.23 s as above), while the whole data ranges from 0 to 2.5.

Fig. 3 shows the curves of the true (projected) states and the states computed with the model (reduced) for the training and validation data. The model states match the system dynamics for the training sample as well as for the

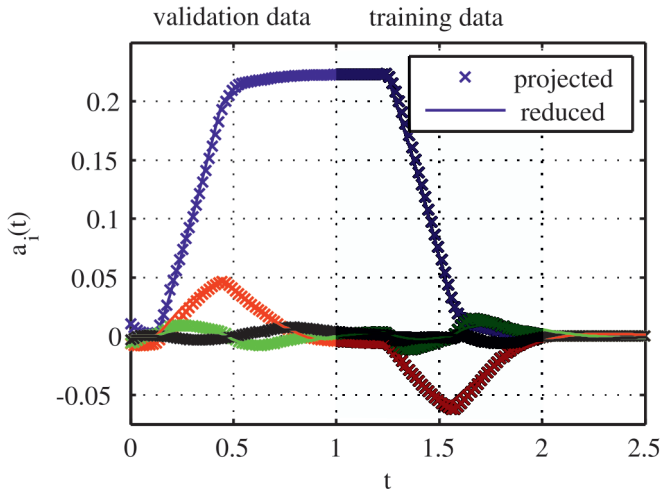

Fig. 3. Comparison of the projected and the model based coefficients for the whole simulation-time

validation samples. With four modes more than 90% of the relative information content of the snapshot ensemble can be represented. This number of modes is used for the reduced order model. Together with the time average flow field mode and the actuation mode, the reduced order model comprises six states in total. The Fluent simulation has over seven million states.

5. CONTROLLER-DESIGN AND PERFORMANCE

After the derivation of a reduced model for the given plant, it is possible to design a model predictive controller, which explicitly uses this model.

5.1 Controller and Estimator

The controller solves a finite horizon open-loop control problem in every time step and applies the first value of the calculated optimal control sequence to the plant. For that purpose the nonlinear continuous time model is linearized and discretized in each time step. To take advantage of the available continuous time description of the plant, the free system response is predicted using the full nonlinear model. To secure stationary accuracy the error in the prediction at the point of measurement $d_0 = y - y_{pred}$ is fed back. The reference trajectory is shifted with this value so that

$$\text{ref} + d_0 - y = \text{ref} + (y - y_{pred}) - y = \text{ref} - y_{pred} \quad (27)$$

holds. In this formulation the minimum of $\text{ref} - y_{pred} - d_0$ (the predicted output and the shifted reference trajectory) leads to a minimum of $\text{ref} - y$, which is the desired goal of the control. Since the model predictive controller needs the state of the system an estimator was implemented in addition. To unify the time continuous plant with the discrete output and input variables a hybrid extended Kalman filter (see e.g. Simon [2006]) was used. The estimation problem could be solved using only the controlled variable (temperature at $(20\,\text{m}, 1.2\,\text{m})$) as measurement.

5.2 Results

This controller has been tested in a closed loop simulation using the CFD simulation as plant. As the controller has been implemented in Matlab, a coupling of Matlab with the CFD-Solver Fluent has to be designed as closed-loop interface. This has been done using the possibility to change boundary conditions in Fluent via a user defined function (udf). Matlab generates after every time step a new file containing this udf with the new boundary conditions computed by the controller. Fluent is run as batch process in Matlab and simulates the plant with the new boundary condition one time step and hands the measurement information, that is the temperature value at the position (20 m 1.2 m), to the controller.
In order to evaluate the performance, the controller has been analyzed regarding reference action and disturbance rejection. The measurement of this output has been disturbed with a white measurement noise with $\sigma = 0.1\,\text{K}$ The reference trajectory ranges from 1800 K to 2050 K, which doubles the operating range from 1925 K to 2050 K covered by the data used for training the model. In spite of the big range the controller was able to follow the reference as shown in Fig. 4.

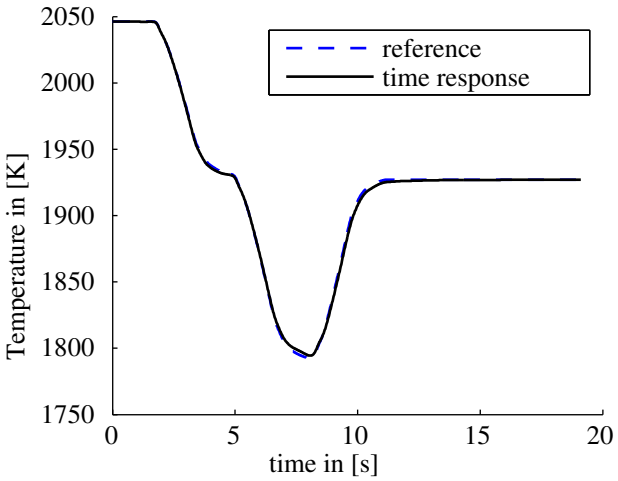

Fig. 4. Time response for varying reference trajectory

Second the controller received an stationary reference value. Then the mass flow inlet has been increased by 20% as an unknown disturbance. This perturbation is neither known to the controller nor to the model, because it did not occur in the snapshots. But the controller has the ability to compensate the disturbance as shown in Fig. 5. The corresponding values for the input of the plant are shown in Fig. 6. The values are scaled with the factor 2.5 kg/s, so that the maximum change of the input is roughly 1.2 kg/s. The amplitudes are in an acceptable range regarding the amplitude of the disturbance. The shown values are not the input variable to the model w, but the value of the boundary condition u.

6. CONCLUSION AND OUTLOOK

The applied procedure is able to produce a reduced model for the model predictive controller, which is good enough to enable a good controller performance. Due to the POD-Galerkin procedure the polynomial order of the model is known and the number of states is small. This allows an optimization of the model coefficients to receive an accurate model. Drawbacks are, that the model only

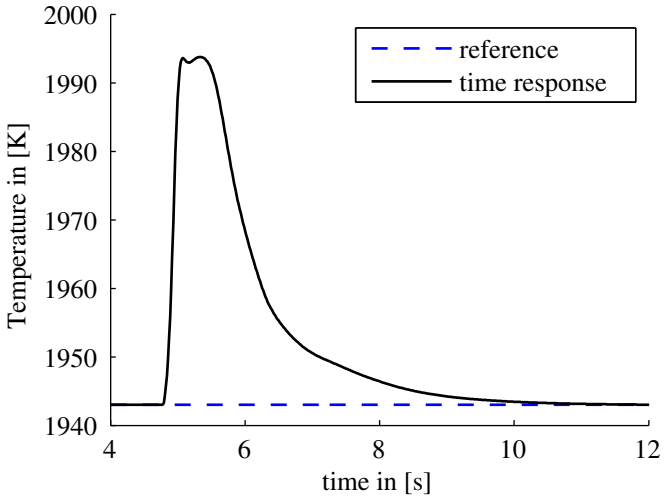

Fig. 5. Time response for a disturbance in form of a step

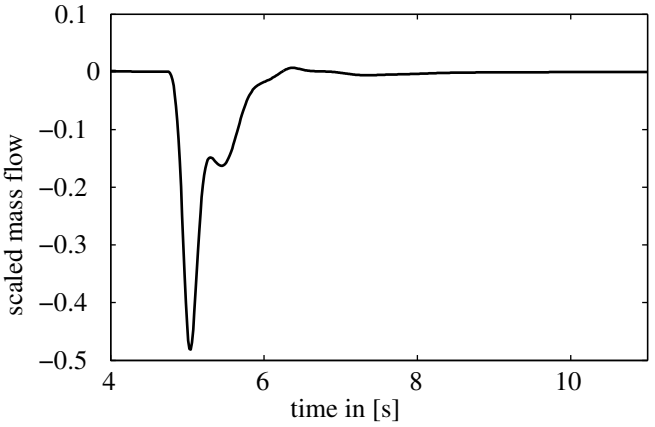

Fig. 6. Value of the input to reject the disturbance

represents the dynamic information in the operating range due to the linearization in temperature and the need of snapshot data. Also the optimization of the coefficients may not represent the real physics like an analytical computation based on the modes.
Further steps are to integrate the $k-\epsilon$ turbulence model into the equations to improve the Galerkin projection. Also an analytical computation of the model coefficients and a comparison with the optimized coefficients is needed. Finally, an integration of disturbances into the data used for the POD is desired to give the model knowledge about characteristic disturbances and by that improve their rejection.

REFERENCES

Inc. ANSYS. *ANSYS Fluent*, 2011.

J. Baker and P. D. Christofides. Nonlinear control of incompressible fluid flows. In *Proceedings of the 38th Conference on Decision & Control*, Phoenix, Arizona, USA, 1999.

L. Cordier, B. Abou El Majd, and J. Favier. Calibration of POD reduced-order models using Tikhonov regularization. *International Journal for Numerical Methods in Fluids*, (63):269–296, 2009.

M. Couplet, C. Basdevant, and P. Sagaut. Calibrated reduced-order POD-Galerkin system for fluid flow modelling. *Journal of Computational Physics*, (207):192–220, 2005.

X. Gloerfelt. Compressible proper orthogonal decomposition/Galerkin reduced-order model of self sustained oscillations in a cavity. *Physics of Fluids*, (20), 2008.

W.R. Graham, J. Peraire, and K.Y. Tang. Optimal control of vortex shedding using low-order models. Part 1 - Open loop model development. *International Journal for Numerical Methods in Engineering*, 44:945–972, 1999.

P. Holmes, J. Lumley, and G. Berkooz. *Turbulence, Coherent Structures, Dynamical Systems and Symmertry*. Cambridge University Press, 1st edition, 1996.

A. Iollo, S. Lanteri, and J. Désidéri. Stability Properties of POD-Galerkin approximations for the compressible Navier-Stokes-equations. *Theoretical and Computational Fluid Dynamics*, 13:377–396, 2000.

K. Kunisch and S. Volkwein. Control of the burgers equation by a reduced-order approach using proper orthogonal decomposition. *Journal of Optimization Theory and Applications*, 102(2):345–371, 1999.

X. Ma and G.E. Karniadakis. A low-dimensional model for simulating three-dimensional cylinder flow. *J. Fluid Mech.*, 458:181–190, 2002.

C.W. Rowley, T. Colonius, and R.M. Murray. Model reduction for compressible flows using POD and Galerkin projection. *Physica D*, 189:115–129, 2004.

D. Simon. *Optimal State Estimation*. John Wiley & Sons, 1st edition, 2006.

L. Sirovich. Turbulence and the dynamics of coherent structures part I: Coherent structures. *Quarterly of Applied Mathematics*, (45,3):561–571, 1987.

Appendix A. EXEMPLARY COMPUTATION FOR THE REDUCED MODEL

To compute the Matrix Ξ_j first the related ODE has to be set up. With the notation $\frac{\partial}{\partial x_1} = \partial_1$ and $\frac{\partial}{\partial x_2} = \partial_2$

$$\dot{\xi} = \left(\frac{\dot{1}}{\rho}\right) = -\frac{\dot{\rho}}{\rho^2} = \frac{1}{\rho^2}\left(\rho\partial_1 u + \rho\partial_2 v + u\partial_1\rho + v\partial_2\rho\right)$$
$$= \xi\partial_1 u + \xi\partial_2 v - u\partial_1\xi - v\partial_2\xi. \tag{A.1}$$

follows. Using (19), (23) and (24) further

$$\begin{aligned}\langle\dot{\xi},\varphi_j^I\rangle &= \langle\xi\partial_1 u + \xi\partial_2 v - u\partial_1\xi - v\partial_2\xi, \varphi_j^I\rangle \\ &= \langle\sum_{i=1}^{N+2} a_i\varphi_i^I \sum_{k=1}^{N+2} a_k\partial_1\varphi_k^{II} + \sum_{i=1}^{N+2} a_i\varphi_i^I \sum_{k=1}^{N+2} a_k\partial_2\varphi_k^{III} \\ &\quad - \sum_{i=1}^{N+2} a_i\partial_1\varphi_i^I \sum_{k=1}^{N+2} a_k\varphi_k^{II} - \sum_{i=1}^{N+2} a_i\partial_1\varphi_i^I \sum_{k=1}^{N+2} a_k\varphi_k^{III}, \varphi_j^I\rangle \\ &= (a_1\ \cdots\ a_{N+2})\left(\Xi_{ik}^j\right)_{ik}(a_1\ \cdots\ a_{N+2})^{\mathrm{T}} = a^{\mathrm{T}}\Xi^j a\end{aligned}$$

holds with

$$\Xi_{ik}^j = \langle\varphi_i^I\partial_1\varphi_k^{II} + \varphi_i^I\partial_2\varphi_k^{III} - \partial_1\varphi_i^I\varphi_k^{II} - \partial_1\varphi_i^I\varphi_k^{III}, \varphi_j^I\rangle. \tag{A.2}$$

An ODE for the coefficient a_j is gathered via the equation

$$\langle\dot{y},\varphi_j\rangle = \langle\sum_{i=1}^{N+2}\dot{a}_i\varphi_i,\varphi_j\rangle = \dot{a}_j + \langle\sum_{i=N+1}^{N+2}\dot{a}_i\varphi_i,\varphi_j\rangle = \dot{a}_j - wg_j$$
$$= \langle\dot{\xi},\varphi_j^I\rangle + \cdots + \langle\dot{\chi},\varphi_j^{VI}\rangle.$$